

Side weir simulation using two different support vector machine methods

Hossein Bonakdari

Amir Hossein Zaji

Abstract—Determining the accurate discharge coefficient is a crucial process in side weirs design. Because of the higher performance modified-shape side weirs are used extensively in practical situations. The discharge coefficients of modified-shape side weirs are complex because they are related to various geometric and hydraulic conditions, such as the weir's height (w), included angle (θ), length (L), and the upstream Froude number (F_1). In this study, Support Vector Regression (SVR) was used to predict the discharge coefficient of a modified-shape, labyrinth side weir. Polynomial and radial basis functions were investigated as kernel functions. Instead of minimizing the training error, the Polynomial SVR (Poly-SVR) and the Radial Basis Function SVR (RBF-SVR) minimize the generalization error in the training process. Investigation of the performance of the proposed method showed that both Poly-SVR and RBF-SVR provided accurate predictions, and the generalization-based SVR was used successfully in complex hydraulic prediction problems.

Keywords—discharge coefficient, kernel function, modified-shape labyrinth side weir, soft computing, support vector regression

I. INTRODUCTION

Side weirs have been used extensively in hydraulic and environmental engineering as a substantial part of controlling and dividing flow structures. The first mathematical study of side weirs was done by De Marchi [1]. The author assumed that the specific energy was constant upstream and downstream from the side weirs, and presented the following equation:

$$-\frac{dQ}{dx} = \frac{2}{3} Cd \sqrt{2g} (y - w)^{1/5} \quad (1)$$

where Cd is the discharge coefficient, w weir height, y flow depth, and dQ/dx the variation of discharge with respect to the spatial coordinate.

Hossein Bonakdari Professor, is with the Department of Civil Engineering Razi University Kermanshah, Iran (e-mail: bonakdari@yahoo.com). Amir Hossein Zaji Ph.D. candidate, is with the Department of Civil Engineering Razi University Kermanshah, Iran (e-mail: amirzaji@gmail.com)

The first side weirs that were investigated had a rectangular shape. Characteristics of rectangular side weirs, specially their discharge coefficients, have been studied extensively [2-7].

When the discharge of the diverted flow exceeds the capacity of the side weir, the most effective strategy is to

increase the length of the side weir. The width of the branch channel is related to the length of the side weir, and increasing the length of the side weir results in an increase in the length of the branch channel. The modification of this structure is extremely costly, and when there is a limitation in width of the branch channel, it is impossible. To increase the capacity of the side weir, shape modification is another alternative. Numerous studies have indicated that modifying the shape of the side weir could increase its capacity and increase the discharge coefficient by a factor ranging from 1.5 to 4.5 [8-13].

The discharge coefficients of modified-shape, labyrinth side weirs are related to various input parameters, and, hence, they have a complex nature. Therefore, soft-computing methods have been used extensively to predict the discharge coefficients of side weirs [8, 14-16]. Support vector regression (SVR) is a powerful learning algorithm that is used extensively in various fields, including hydraulic and hydrology engineering [17-19].

The discharge coefficient of a modified, labyrinth side weir is affected by various geometric parameters, such as the weir's height, length, and included angle, as well as hydraulic parameters, such as upstream Froude number and the depth of the flow. By using efficient parameters, ten non-dimensional input variables were performed and used in numerical models. The discharge coefficients were investigated and modeled with two high-performance predictive models, i.e., Poly-SVM and RBF-SVM, and the obtained results were compared.

II. MATERIALS AND METHODS

A. Experimental dataset

An experimental study conducted by Borghei and Parvaneh [20] was used to calibrate and verify the Poly-

SVR and RBF-SVR models. Fig. 1 shows a schematic illustration of the experimental flume. The experiments were performed in a channel made of glass, and the length (L), height (h), and width (w) of the channel were 11, 0.66, and 0.4 m, respectively.

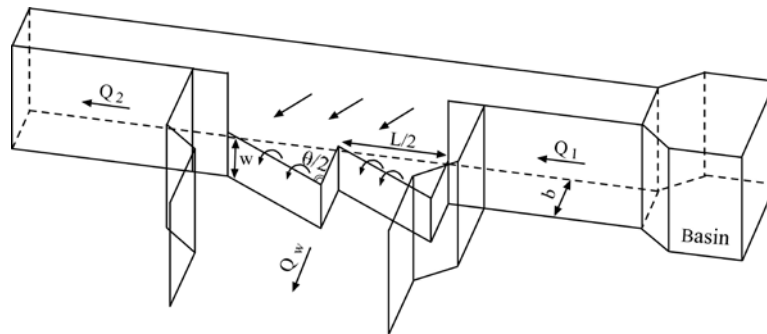


Fig. 1. Modified labyrinth side weir [20]

Various hydraulic and geometrical situations of the shape of the modified weir were examined by changing the geometric conditions of the weir, including the angle, θ ; the weir's length, L ; and the weir's height, w . Hydraulic conditions were also changed, including the upstream Froude number, F_1 , and the upstream flow depth, y_1 . Table I shows the various values of the variation of side weir's parameters.

B. Support vector regression

Support Vector Regression (SVR) is a subset of neural network methods, and it provides better predictions than other neural network methods [21-24]. Unlike the other machine-learning methods that use local training error in the training process, SVR conducts the training by minimizing the generalization error of the upper band [25]. Detailed descriptions of the SVR method are given in Rajasekaran, et al. [26] and Yang, et al. [27].

In the SVR procedure, a non-linear mapping is done, so that the input parameters (x), are mapped into a multi-dimensional future space. The multi-dimensionality of the future space leads to extreme increases in the computational cost and time. The computations can be done by a simple, linear function, but, for complex problems, such as predicting the discharge coefficient, a more hypothetical

space is required. A schematic kernel function is shown as follows, such that for all $x, z \in X$.

$$K(x, z) = \langle \phi(x), \phi(z) \rangle \quad (2)$$

To construct a learning machine, different kernels can be

used to map the input variables into different types of non-linear decision surfaces. Two common types of learning machines are the Polynomial Function (PF) and the Radial Basis Function (RBF), which are defined as follows:

$$K(x, x_i) = [(x \times x_i) + 1]^d \quad (3)$$

$$K(x, x_i) = \exp[-\gamma |x - x_i|^2] \quad (4)$$

where d represents the polynomial's dimensions, and γ is the RBF constant. To determine the discharge coefficient of a modified-shape, labyrinth side weir, two types of SVMs (SVM-Poly and SVM-RBF) were investigated and examined. The performance of each standard SVM model was related directly to the optimum selection of the SVM's parameters. For SVR-RBF, the SVM's parameters are C , γ , and ε , and for SVR-Poly, the SVM's parameters are C , d , and ε . These parameters are not known at the beginning of the modelling; they must be determined in the model calibration process.

III. RESULTS

TABLE I. THE DIFFERENT GEOMETRIC AND HYDRAULIC PARAMETERS USED FOR THE MODIFIED LABYRINTH SIDE WEIR [20]

$\theta/2$ (°)	L (m)	w (mm)	w/Y_1	Q_1 (m ³ /s)	F_1	Number of runs
30	0.3	50,75,100,150	0.46-0.83	0.019-0.030	0.19-0.96	40
	0.4	50,75,100,150				
45	0.3	50,75,100,150	0.46-0.83	0.019-0.030	0.19-0.96	55
	0.4	50,75,100,150				
	0.6	50,100,150				
60	0.3	50,75,100,150	0.46-0.83	0.019-0.030	0.19-0.96	50
	0.4	50, 100,150				
	0.6	50, 100,150				
70	0.3	50,75,100,150	0.46-0.83	0.019-0.030	0.19-0.96	55
	0.4	50,75,100,150				
	0.6	50,100,150				

TABLE II. STATISTICAL ERRORS BETWEEN SVR AND SVR-FF IN THE TRAINING AND TEST DATASETS

Model	Training process			Testing process			SVR parameters		
	RMSE	MAE	% δ	RMSE	MAE	% δ	C	ε	d (Poly) γ (RBF)
Poly-SVR	0.037	0.027	4.250	0.056	0.045	6.289	100	0.001	1
RBF-SVR	0.026	0.013	2.118	0.081	0.066	9.078	100	0.001	0.01

The SVR method was used in this study to develop a high-performance model for predicting the discharge coefficient of a modified-shape, labyrinth side weir. The non-dimensional input variables of the models were w/b , y_1/b , L/b , w/y_1 , w/L , y_1/L , $\sin(\theta/2)$, F_1 , $F_1/\sin(\theta/2)$ and $w \times \sin(\theta/2)/y_1$, and the output variable was Cd . Polynomial and RBF were used as kernel functions for predicting the discharge coefficient. The SVR's performance depended directly on the selection of the optimum parameters for the model. Each of the Poly-SVR and RBF-SVR models must have three parameters specified, i.e., C , ε , and d for the polynomial kernel SVR and C , ε , and γ for the RBF kernel SVR. For this problem, the default value of $\varepsilon = 0.001$ seemed to be appropriate. To determine the optimum values of C , d and γ , several trial and error calculations were conducted with different combinations of C and d for Poly-

SVR and different combinations of C and γ for RBF-SVR [28]. The optimal values of the parameters of Poly-SVR and RBF-SVR and performance of each model the in training and testing process are provided in Table II, which shows that the Poly-SVR model had a small Root Mean Square Error (RMSE) of 0.037 in training and 0.056 in the testing procedure. However, RBF-SVR had very small RMSE values of 0.026 in training and 0.081 in the testing procedure. Because of the proximity of the results of the Poly-SVR in test and train procedures, this model was more trustable than RBF-SVR model. Despite the higher performance of the RBF-SVR in the training procedure, it is preferred to use a model that has about the same performance for the training and test samples. Fig. 2 shows scatter plots of the Poly-SVR and RBF-SVR models. The figure shows that the Poly-SVR model does not trapped in

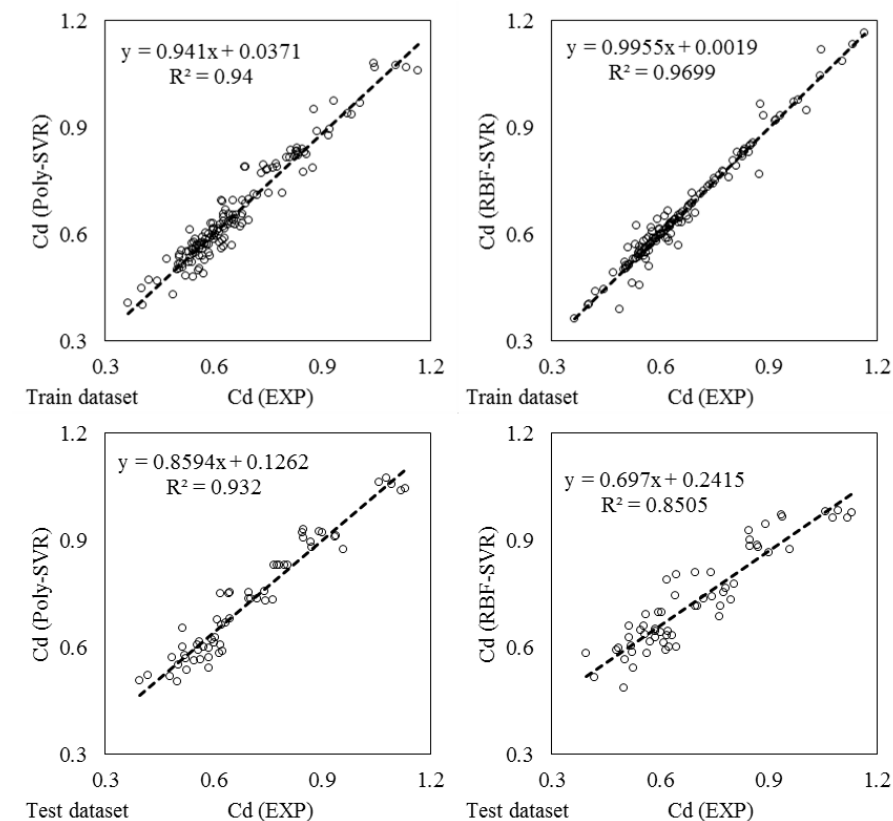


Fig. 2. Scatter plot of Poly-SVR and RBF-SVR methods in the training and test datasets

the over- and under-estimation, i.e., the linear trend line equation of $y = C_1x + C_2$ has a C_1 value close to 1 and a C_2 value close to 0. So, the trend line of the Poly-SVR model almost fit the 45° ideal fit line. However, even though the RBF-SVR model almost fit linear trend line to the ideal fit line in the training samples, it did not perform very well near the ideal line in the test samples, with a C_1 value and a C_2 value of 0.697 and 0.241, respectively.

IV. CONCLUSIONS

Polynomial and Radial Basis Function Support Vector Regression methods were used to model the discharge coefficient of a modified-shape side weir. The discharge coefficient of the side weir depended on w , L , θ , y_1 , b and F_1 . By using these parameters, ten different, non-dimensional input parameters were performed and two models, i.e., Poly-SVR and RBF-SVR, were used to predict the discharge coefficient. The results showed that the Poly-SVR model had high and reasonable accuracy, and, because of the close correlation between the results of the training and test performance, it can be used with confidence in practical situations.

REFERENCES

- [1] G. De Marchi, "Saggio di teoria del funzionamento degli stramazzi laterali," *L'Energia elettrica*, vol. 11, pp. 849-860, 1934.
- [2] R. Singh, D. Manivannan, and T. Satyanarayana, "Discharge coefficients of rectangular side weirs," *J. Irrig. Drain. Eng.*, vol. 120, pp. 814-819, 1994.
- [3] P. K. Swamee, S. K. Pathak, and M. S. Ali, "Side weir analysis using elementary discharge coefficient," *J. Irrig. Drain. Eng.*, vol. 120, pp. 742-755, 1994.
- [4] Y. Muslu, "Numerical analysis of lateral weir flow," *J. Irrig. Drain. Eng.*, vol. 127, pp. 246-253, 2001.
- [5] M. Ghodsian, "Supercritical flow over a rectangular side weir," *Can. J. Civ. Eng.*, vol. 30, pp. 596-600, 2003.
- [6] Y. Muslu, H. Tozlu, and E. Yuksel, "Effect of lateral water surface profile on side weir discharge," *J. Irrig. Drain. Eng.*, vol. 129, pp. 371-375, 2003.
- [7] E. Yuksel, "Effect of specific energy variation on lateral overflows," *Flow. Meas. Instrum.*, vol. 15, pp. 259-269, 2004.
- [8] O. Bilhan, M. Emin Emiroglu, and O. Kisi, "Application of two different neural network techniques to lateral outflow over rectangular side weirs located on a straight channel," *Adv. Eng. Software.*, vol. 41, pp. 831-837, 2010.
- [9] M. E. Emiroglu, N. Kaya, and H. Agaccioglu, "Discharge capacity of labyrinth side weir located on a straight channel," *J. Irrig. Drain. Eng.*, vol. 136, pp. 37-46, 2010.
- [10] M. C. Aydin and M. E. Emiroglu, "Determination of capacity of labyrinth side weir by CFD," *Flow. Meas. Instrum.*, vol. 29, pp. 1-8, 2013.
- [11] M. Mirnaseri and A. Emadi, "Hydraulic performance of combined flow rectangular labyrinth weir-gate," *Middle East J. Sci. Res.*, vol. 18, pp. 1335-1342, 2013.
- [12] C. Bautista-Capetillo, O. Robles, H. Junez-Ferreira, and E. Playan, "Discharge coefficient analysis for triangular sharp-crested weirs using low-speed photographic technique," *J. Irrig. Drain. Eng.*, vol. 140, 2014.
- [13] M. Emin Emiroglu, M. Cihan Aydin, and N. Kaya, "Discharge Characteristics of a Trapezoidal Labyrinth Side Weir with One and Two Cycles in Subcritical Flow," *J. Irrig. Drain. Eng.*, vol. 140, 2014.
- [14] M. E. Emiroglu, O. Bilhan, and O. Kisi, "Neural networks for estimation of discharge capacity of triangular labyrinth side-weir located on a straight channel," *Expert. Sys. Appl.*, vol. 38, pp. 867-874, 2011.
- [15] O. Kisi, M. Emin Emiroglu, O. Bilhan, and A. Guven, "Prediction of lateral outflow over triangular labyrinth side weirs under subcritical conditions using soft computing approaches," *Expert. Sys. Appl.*, vol. 39, pp. 3454-3460, 2012.
- [16] F. Onen, "Prediction of Scour at a Side-Weir with GEP, ANN and Regression Models," *Arab. J. Sci. Eng.*, vol. 39, pp. 6031-6041, 2014.
- [17] T. Asefa, M. Kemblowski, M. McKee, and A. Khalil, "Multi-time scale stream flow predictions: The support vector machines approach," *J. Hydrol.*, vol. 318, pp. 7-16, 2006.
- [18] Y. Ji and S. Sun, "Multitask multiclass support vector machines: Model and experiments," *Pattern. Recogn.*, vol. 46, pp. 914-924, 2013.
- [19] S. Sun, "A survey of multi-view machine learning," *Neural. Comput. Appl.*, vol. 23, pp. 2031-2038, 2013.
- [20] S. M. Borghei and A. Parvaneh, "Discharge characteristics of a modified oblique side weir in subcritical flow," *Flow. Meas. Instrum.*, vol. 22, pp. 370-376, 2011.
- [21] V. Vapnik, S. E. Golowich, and A. Smola, "Support vector method for function approximation, regression estimation, and signal processing," in *10th Annual Conference on Neural Information Processing Systems*, NIPS 1996, Denver, CO, 1997, pp. 281-287.
- [22] V. Vapnik, *The nature of statistical learning theory*: springer, 2000.
- [23] C. Huang, L. S. Davis, and J. R. G. Townshend, "An assessment of support vector machines for land cover classification," *Int. J. Remote Sens.*, vol. 23, pp. 725-749, 2002.
- [24] A. H. Sung and S. Mukkamala, "Identifying important features for intrusion detection using support vector machines and neural networks," *Proc. Int. Sym. Appl. Internet.*, pp. 209-216, 2003.
- [25] S. Shamshirband, D. Petkovic, H. Javidnia, and A. Gani, "Sensor data fusion by support vector regression methodology; a comparative study," *Sensors. J.*, IEEE, vol. PP, pp. 1-1, 2014.
- [26] S. Rajasekaran, S. Gayathri, and T. L. Lee, "Support vector regression methodology for storm surge predictions," *Ocean. Eng.*, vol. 35, pp. 1578-1587, 2008.
- [27] H. Yang, K. Huang, I. King, and M. R. Lyu, "Localized support vector regression for time series prediction," *Neurocomputing.*, vol. 72, pp. 2659-2669, 2009.
- [28] M. Pal, N. K. Singh, and N. K. Tiwari, "Support vector regression based modeling of pier scour using field data," *Eng. Appl. Artif. Intell.*, vol. 24, pp. 911-916, 2011.